Matrix Converters: A Technology Review

Patrick W. Wheeler, *Member, IEEE*, José Rodríguez, *Senior Member, IEEE*, Jon C. Clare, *Member, IEEE*, Lee Empringham, *Member, IEEE*, and Alejandro Weinstein

***Abstract*—The matrix converter is an array of controlled semiconductor switches that connects directly the three-phase source to the three-phase load. This converter has several attractive features that have been investigated in the last two decades. In the last few years, an increase in research work has been observed, bringing this topology closer to the industrial application. This paper presents the state-of-the-art view in the development of this converter, starting with a brief historical review. An important part of the paper is dedicated to a discussion of the most important modulation and control strategies developed recently. Special attention is given to present modern methods developed to solve the commutation problem. Some new arrays of power bidirectional switches integrated in a single module are also presented. Finally, this paper includes some practical issues related to the practical application of this technology, like overvoltage protection, use of filters, and ride-through capability.**

***Index Terms*—AC–AC power conversion, converters, matrix converters.**

I. Introduction

AMONG THE MOST desirable features in power frequency changers are the following:

1) simple and compact power circuit;
2) generation of load voltage with arbitrary amplitude and frequency;
3) sinusoidal input and output currents;
4) operation with unity power factor for any load;
5) regeneration capability.

These ideal characteristics can be fulfilled by matrix converters, and this is the reason for the tremendous interest in the topology.

The matrix converter is a forced commutated converter which uses an array of controlled bidirectional switches as the main power elements to create a variable output voltage system with unrestricted frequency. It does not have any dc-link circuit and does not need any large energy storage elements.

The key element in a matrix converter is the fully controlled four-quadrant bidirectional switch, which allows high-frequency operation. The early work dedicated to unrestricted frequency changers used thyristors with external forced commutation circuits to implement the bidirectional controlled switch [1]–[4]. With this solution, the power circuit was bulky and the performance was poor.

The introduction of power transistors for implementing the bidirectional switches made the matrix converter topology more attractive [5]–[9]. However, the real development of matrix converters starts with the work of Venturini and Alesina published in 1980 [10], [11]. They presented the power circuit of the converter as a matrix of bidirectional power switches and they introduced the name "matrix converter." One of their main contributions is the development of a rigorous mathematical analysis to describe the low-frequency behavior of the converter, introducing the "low-frequency modulation matrix" concept. In their modulation method, also known as the direct transfer function approach, the output voltages are obtained by the multiplication of the modulation (also called transfer) matrix with the input voltages.

A conceptually different control technique based on the "fictitious dc link" idea was introduced by Rodriguez in 1983 [12]. In this method, the switching is arranged so that each output line is switched between the most positive and most negative input lines using a pulsewidth modulation (PWM) technique, as conventionally used in standard voltage-source inverters (VSIs). This concept is also known as the "indirect transfer function" approach [15]. In 1985–1986, Ziogas *et al.* published [13] and [40], which expanded on the "fictitious dc link" idea of Rodriguez and provided a rigorous mathematical explanation. In 1983, Braun [16], and in 1985 Kastner and Rodriguez [18], introduced the use of space vectors in the analysis and control of matrix converters. In 1989, Huber *et al.* published the first of a series of papers [14], [41]–[45] in which the principles of space-vector modulation (SPVM) were applied to the matrix converter modulation problem [17].

The modulation methods based on the Venturini approach are known as "direct methods," while those based on the "fictitious dc link" are known as "indirect methods."

It was experimentally confirmed by Kastner and Rodriguez in 1985 [18] and Neft and Schauder in 1992 [19] that a matrix converter with only nine switches can be effectively used in the vector control of an induction motor with high quality input and output currents. However, the simultaneous commutation of controlled bidirectional switches used in matrix converters is very difficult to achieve without generating overcurrent or overvoltage spikes that can destroy the power semiconductors. This fact limited the practical implementation and negatively affected the interest in matrix converters. Fortunately, this major problem has been solved with the development of several multistep commutation strategies that allow safe operation of the switches. In 1989, Burany [36] introduced the later-named "semi-soft current commutation" technique. Other interesting commutation

Manuscript received April 14, 2001; revised August 30, 2001. Abstract published on the Internet January 9, 2002.

P. W. Wheeler, J. Clare, and L. Empringham are with the Power Electronics, Machines and Control Group, School of Electrical and Electronic Engineering, University of Nottingham, Nottingham, NG7 2RD, U.K. (e-mail: Jon.Clare@nottingham.ac.uk; Pat.Wheeler@nottingham.ac.uk; le@eee.nottingham.ac.uk).

J. Rodríguez and A. Weinstein are with the Departamento de Electronica, Universidad Técnica Federico Santa María, Valparaiso, Chile (e-mail: jrp@elo.utfsm.cl).

Publisher Item Identifier S 0278-0046(02)02895-2.

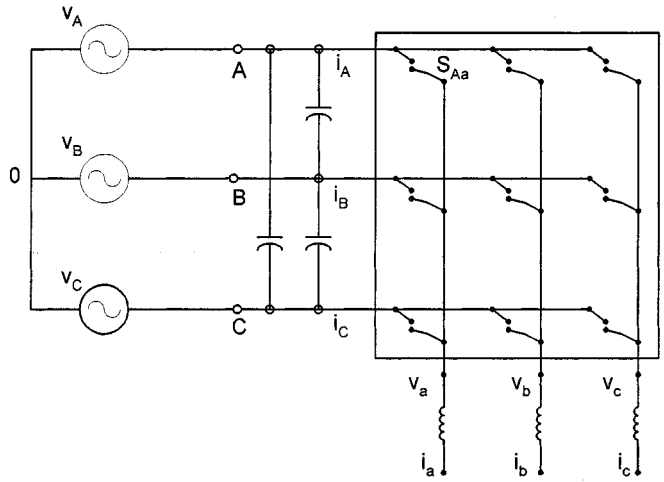

Fig. 1. Simplified circuit of a 3 × 3 matrix converter.

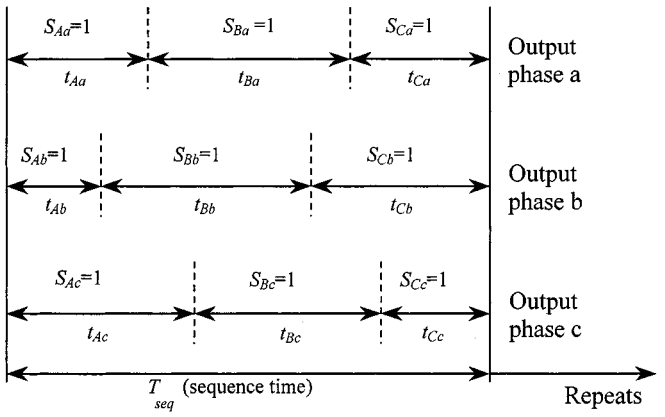

Fig. 2. General form of switching pattern.

strategies were introduced by Ziegler *et al.* [22], [37] and Clare and Wheeler in 1998 [21], [38] [39].

Today, the research is mainly focused on operational and technological aspects: reliable implementation of commutation strategies [20]; protection issues [23], [24]; implementation of bidirectional switches and packaging [25], [26]; operation under abnormal conditions; ride-through capability [28]; and input filter design [29], [30].

The purpose of this paper is to give a review of key aspects concerning matrix converter operation and to establish the state of the art of this technology. It begins by studying the topology of the matrix converter, the main control techniques, the practical implementation of bidirectional switches and commutation strategies. Finally, some practical issues and challenges for the future are discussed.

II. Fundamentals

The matrix converter is a single-stage converter which has an array of $m \times n$ bidirectional power switches to connect, directly, an m-phase voltage source to an n-phase load. The matrix converter of 3 × 3 switches, shown in Fig. 1, has the highest practical interest because it connects a three-phase voltage source with a three-phase load, typically a motor.

Normally, the matrix converter is fed by a voltage source and, for this reason, the input terminals should not be short circuited. On the other hand, the load has typically an inductive nature and, for this reason, an output phase must never be opened.

Defining the switching function of a single switch as [45]

$$S_{Kj} = \begin{cases} 1, & \text{switch } S_{Kj} \text{ closed} \\ 0, & \text{switch } S_{Kj} \text{ open} \end{cases} \quad K = \{A, B, C\} \quad j = \{a, b, c\}. \tag{1}$$

The constraints discussed above can be expressed by

$$S_{Aj} + S_{Bj} + S_{Cj} = 1, \qquad j = \{a, b, c\}. \tag{2}$$

With these restrictions, the 3 × 3 matrix converter has 27 possible switching states [45].

The load and source voltages are referenced to the supply neutral, "0" in Fig. 1, and can be expressed as vectors defined by

$$\mathbf{v_o} = \begin{bmatrix} v_a(t) \\ v_b(t) \\ v_c(t) \end{bmatrix} \quad \mathbf{v_i} = \begin{bmatrix} v_A(t) \\ v_B(t) \\ v_C(t) \end{bmatrix}. \tag{3}$$

The relationship between load and input voltages can be expressed as

$$\left.\begin{bmatrix} v_a(t) \\ v_b(t) \\ v_c(t) \end{bmatrix} = \begin{bmatrix} S_{Aa}(t) & S_{Ba}(t) & S_{Ca}(t) \\ S_{Ab}(t) & S_{Bb}(t) & S_{Cb}(t) \\ S_{Ac}(t) & S_{Bc}(t) & S_{Cc}(t) \end{bmatrix} \begin{bmatrix} v_A(t) \\ v_B(t) \\ v_C(t) \end{bmatrix} \right\} \quad \mathbf{v_0} = \mathbf{T} \cdot \mathbf{v_i} \tag{4}$$

where $\mathbf{T}$ is the instantaneous transfer matrix.

In the same form, the following relationships are valid for the input and output currents:

$$\mathbf{i_i} = \begin{bmatrix} i_a(t) \\ i_b(t) \\ i_c(t) \end{bmatrix} \quad \mathbf{i_o} = \begin{bmatrix} i_A(t) \\ i_B(t) \\ i_C(t) \end{bmatrix} \tag{5}$$

$$\mathbf{i_i} = \mathbf{T}^T \cdot \mathbf{i_o} \tag{6}$$

where $\mathbf{T}^T$ is the transpose matrix of $\mathbf{T}$.

Equations (4) and (6) give the instantaneous relationships between input and output quantities. To derive modulation rules, it is also necessary to consider the switching pattern that is employed. This typically follows a form similar to that shown in Fig. 2.

By considering that the bidirectional power switches work with high switching frequency, a low-frequency output voltage of variable amplitude and frequency can be generated by modulating the duty cycle of the switches using their respective switching functions.

Let $m_{Kj}(t)$ be the duty cycle of switch S_{Kj}, defined as $m_{Kj}(t) = t_{Kj}/T_{\text{seq}}$, which can have the following values:

$$0 < m_{Kj} < 1 \quad K = \{A, B, C\}, \qquad j = \{a, b, c\}. \tag{7}$$

The low-frequency transfer matrix is defined by

$$\mathbf{M}(t) = \begin{bmatrix} m_{Aa}(t) & m_{Ba}(t) & m_{Ca}(t) \\ m_{Ab}(t) & m_{Bb}(t) & m_{Cb}(t) \\ m_{Ac}(t) & m_{Bc}(t) & m_{Cc}(t) \end{bmatrix}. \tag{8}$$

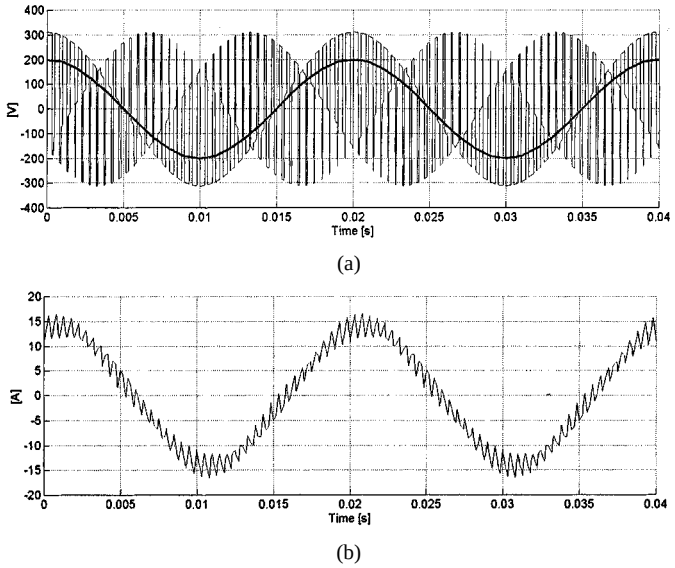

Fig. 3. Typical waveforms. (a) Phase output voltage. (b) Load current.

The low-frequency component of the output phase voltage is given by

$$\overline{\mathbf{v}}_{\mathbf{o}}(t) = \mathbf{M}(t) \cdot \mathbf{v}_{\mathbf{i}}(t). \tag{9}$$

The low-frequency component of the input current is

$$\overline{\mathbf{i}}_{\mathbf{i}} = \mathbf{M}(t)^T \cdot \mathbf{i}_{\mathbf{o}}. \tag{10}$$

Fig. 3 shows simulated waveforms generated by a matrix converter.

III. Bidirectional Switch

The matrix converter requires a bidirectional switch capable of blocking voltage and conducting current in both directions. Unfortunately, there are no such devices currently available, so discrete devices need to be used to construct suitable switch cells.

A. Realization With Discrete Semiconductors

The diode bridge bidirectional switch cell arrangement consists of an insulated gate bipolar transistor (IGBT) at the center of a single-phase diode bridge [19] arrangement as shown in Fig. 4. The main advantage is that both current directions are carried by the same switching device, therefore, only one gate driver is required per switch cell. Device losses are relatively high since there are three devices in each conduction path. The direction of current through the switch cell cannot be controlled. This is a disadvantage, as many of the advanced commutation methods described later require this.

The common emitter bidirectional switch cell arrangement consists of two diodes and two IGBTs connected in antiparallel as shown in Fig. 5(a). The diodes are included to provide the reverse blocking capability. There are several advantages in using this arrangement when compared to the previous example. The first is that it is possible to independently control the direction of the current. Conduction losses are also reduced since only two

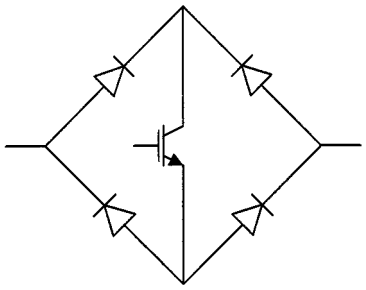

Fig. 4. Diode bridge bidirectional switch cell.

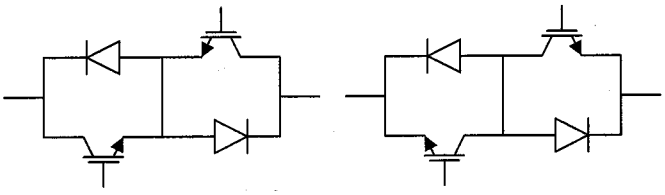

(a) (b)

Fig. 5. Switch cell. (a) Common emitter back to back. (b) Common collecor back to back.

devices carry the current at any one time. One possible disadvantage is that each bidirectional switch cell requires an isolated power supply for the gate drives.

The common collector bidirectional switch cell arrangement is shown in Fig. 5(b). The conduction losses are the same as for the common emitter configuration. An often-quoted advantage of this method is that only six isolated power supplies are needed to supply the gate drive signals [46]. However, in practice, other constraints such as the need to minimize stray inductance mean that operation with only six isolated supplies is generally not viable. Therefore, the common emitter configuration is generally preferred for creating the matrix converter bidirectional switch cells.

Both the common collector and common emitter configurations can be used without the central common connection, but this connection does provide some transient benefits during switching. In the common emitter configuration, the central connection also allows both devices to be controlled from one isolated gate drive power supply.

B. Integrated Power Modules

It is possible to construct the common emitter bidirectional switch cell from discrete components, but it is also possible to build a complete matrix converter in the package style used for standard six-pack IGBT modules. This technology can be used to develop a full matrix converter power circuit in a single package, as shown in Fig. 6. This has been done by Eupec using devices connected in the common collector configuration (see Fig. 7) and is now available commercially [47]. This type of packaging will have important benefits in terms of circuit layout as the stray inductance in the current commutation paths can be minimized.

If the switching devices used for the bidirectional switch have a reverse voltage blocking capability, for example, MOS turn-off thyristor (MTOs), then it is possible to build the bidirectional switches by simply placing two devices in antiparallel.

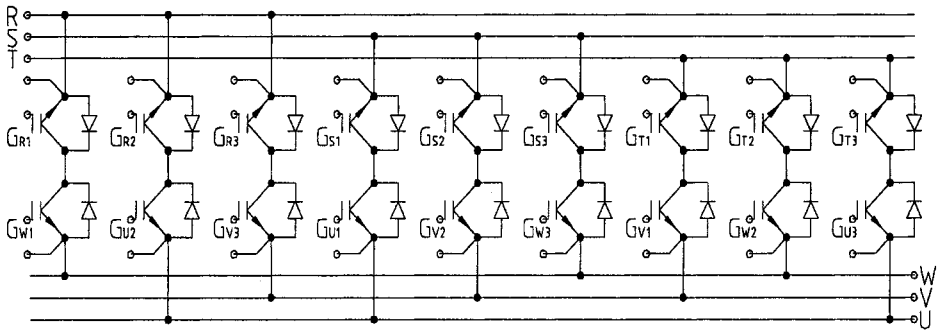

Fig. 6. Power stage of a matrix converter.

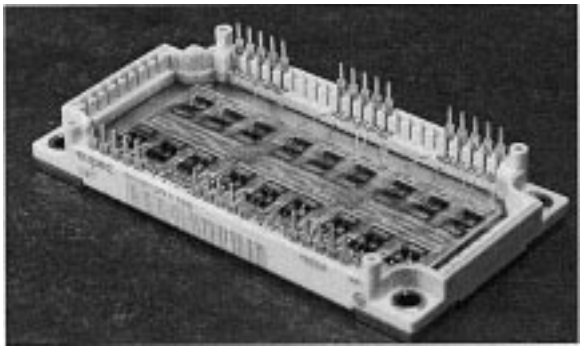

Fig. 7. The Eupec ECONOMAC matrix module.

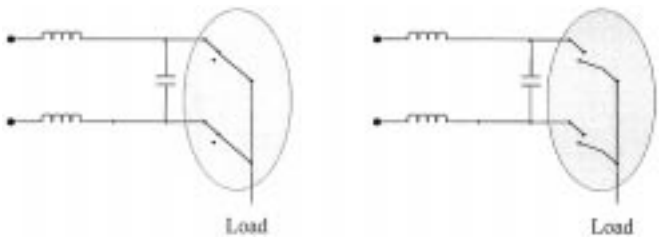

(a) (b)

Fig. 8. (a) Avoid short circuits on the matrix converter input lines. (b) Avoid open circuits on the matrix converter output lines.

This arrangement leads to a very compact converter with the potential for substantial improvements in efficiency.

IV. Current Commutation

Reliable current commutation between switches in matrix converters is more difficult to achieve than in conventional VSIs since there are no natural freewheeling paths. The commutation has to be actively controlled at all times with respect to two basic rules. These rules can be visualized by considering just two switch cells on one output phase of a matrix converter. It is important that no two bidirectional switches are switched on at any instant, as shown pictorially in Fig. 8(a). This would result in line-to-line short circuits and the destruction of the converter due to over currents. Also, the bidirectional switches for each output phase should not all be turned off at any instant, as shown in Fig. 8(b). This would result in the absence of a path for the inductive load current, causing large overvoltages. These two considerations cause a conflict since semiconductor devices cannot be switched instantaneously due to propagation delays and finite switching times.

A. Basic Current Commutation

The two simplest forms of commutation strategy intentionally break the rules given above and need extra circuitry to avoid destruction of the converter. In overlap current commutation, the incoming cell is fired before the outgoing cell is switched off. This would normally cause a line-to-line short circuit but extra line inductance slows the rise in current so that safe commutation is achieved. This is not a desirable method since the inductors used are large. The switching time for each commutation is also greatly increased which may cause control problems.

Dead-time commutation uses a period where no devices are gated, causing a momentary open circuit of the load. Snubbers or clamping devices are then needed across the switch cells to provide a path for the load current. This method is undesirable since energy is lost during every commutation and the bidirectional nature of the switch cells further complicates the snubber design. The clamping devices and the power loss associated with them also results in increased converter volume.

B. Current-Direction-Based Commutation

A more reliable method of current commutation, which obeys the rules, uses a four-step commutation strategy in which the direction of current flow through the commutation cells can be controlled. To implement this strategy, the bidirectional switch cell must be designed in such a way as to allow the direction of the current flow in each switch cell to be controlled.

Fig. 9 shows a schematic of a two-phase to single-phase matrix converter, representing the first two switches in the converter shown in Fig. 1. In steady state, both of the devices in the active bidirectional switch cell are gated to allow both directions of current flow. The following explanation assumes that the load current is in the direction shown and that the upper bidirectional switch (S_{Aa}) is closed. When a commutation to S_{Ba} is required, the current direction is used to determine which device in the active switch is not conducting. This device is then turned off. In this case, device S_{Aa2} is turned off. The device that will conduct the current in the incoming switch is then gated, S_{Ba1} in this example. The load current transfers to the incoming device either at this point or when the outgoing device (S_{Aa1}) is turned off. The remaining device in the incoming switch (S_{Ba2}) is turned on to allow current reversals. This process is shown as a timing

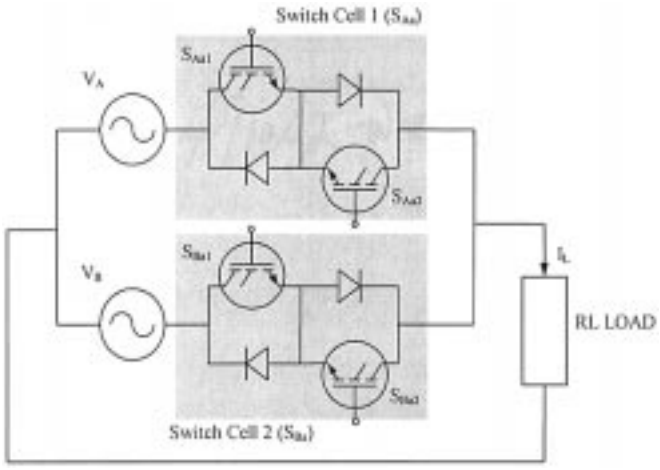

Fig. 9. Two-phase to single-phase matrix converter.

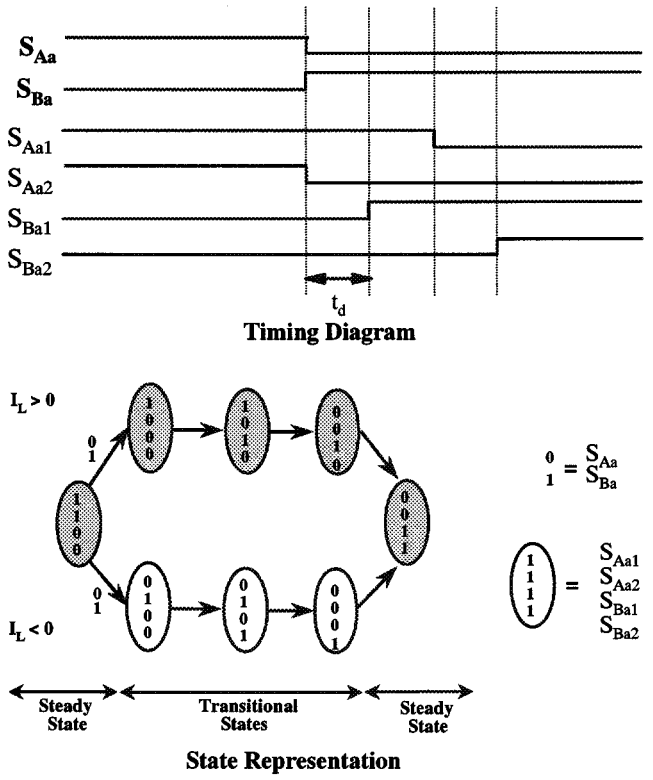

Fig. 10. Four-step semi-soft current commutation between two bidirectional switch cells.

diagram in Fig. 10; the delay between each switching event is determined by the device characteristics.

This method allows the current to commutate from one switch cell to another without causing a line-to-line short circuit or a load open circuit. One advantage of all these techniques is that the switching losses in the silicon devices are reduced by 50% because half of the commutation process is soft switching and, hence, this method is often called "semi-soft current commutation" [46]. One popular variation on this current commutation concept is to only gate the conducting device in the active switch cell, which creates a two-step current commutation strategy [48].

All the current commutation techniques in this category rely on knowledge of the output line current direction. This can be difficult to reliably determine in a switching power converter, especially at low current levels in high-power applications where traditional current sensors such as Hall-effect probes are prone to producing uncertain results. One method that has been used to avoid these potential hazard conditions is to create a "near-zero" current zone where commutation is not allowed to take place, as shown for a two-step strategy in the state representation diagram in Fig. 11. However, this method will give rise to control problems at low current levels and at startup.

To avoid these current measurement problems, a technique for using the voltage across the bidirectional switch to determine the current direction has been developed. This method allows very accurate current direction detection with no external sensors. Because of the accuracy available using this method, a two-step commutation strategy can be employed with deadtimes when the current changes direction, as shown in Fig. 12. This technique has been coupled with the addition of intelligence at the gate drive level to allow each gate drive to independently control the current commutation [21].

C. Relative-Voltage-Magnitude-Based Commutation

There have been two current commutation techniques proposed which use the relative magnitudes of input voltages to calculate the required switching patterns [37], [50]. In the reduction to a two-phase to single-phase converter, these both look identical and resulting timing and phase diagrams are shown in Fig. 13. The main difference between these methods and the current direction based techniques is that freewheel paths are turned on in the input voltage based methods. In "Metzi" current commutation, all the devices are closed except those required to block the reverse voltage [49]. This allows for relatively simple commutation of the current between phases. In [50], only one extra device is closed and the commutation process has to pass between the voltage of the opposite polarity during every commutation, leading to higher switching losses. To successfully implement this type of commutation, it is necessary to accurately measure the relative magnitudes of the input voltages.

D. Soft-Switching Techniques

In many power converter circuits, the use of resonant switching techniques has been proposed and investigated in order to reduce switching losses. In matrix converters, resonant techniques have the additional benefit of solving the current commutation problem. The techniques developed fall into two categories: resonant switch circuits [51], [52] and auxiliary resonant circuits [53]. All these circuits significantly increase the component count in the matrix converter, increase the conduction losses, and most require modification to the converter control algorithm to operate under all conditions.

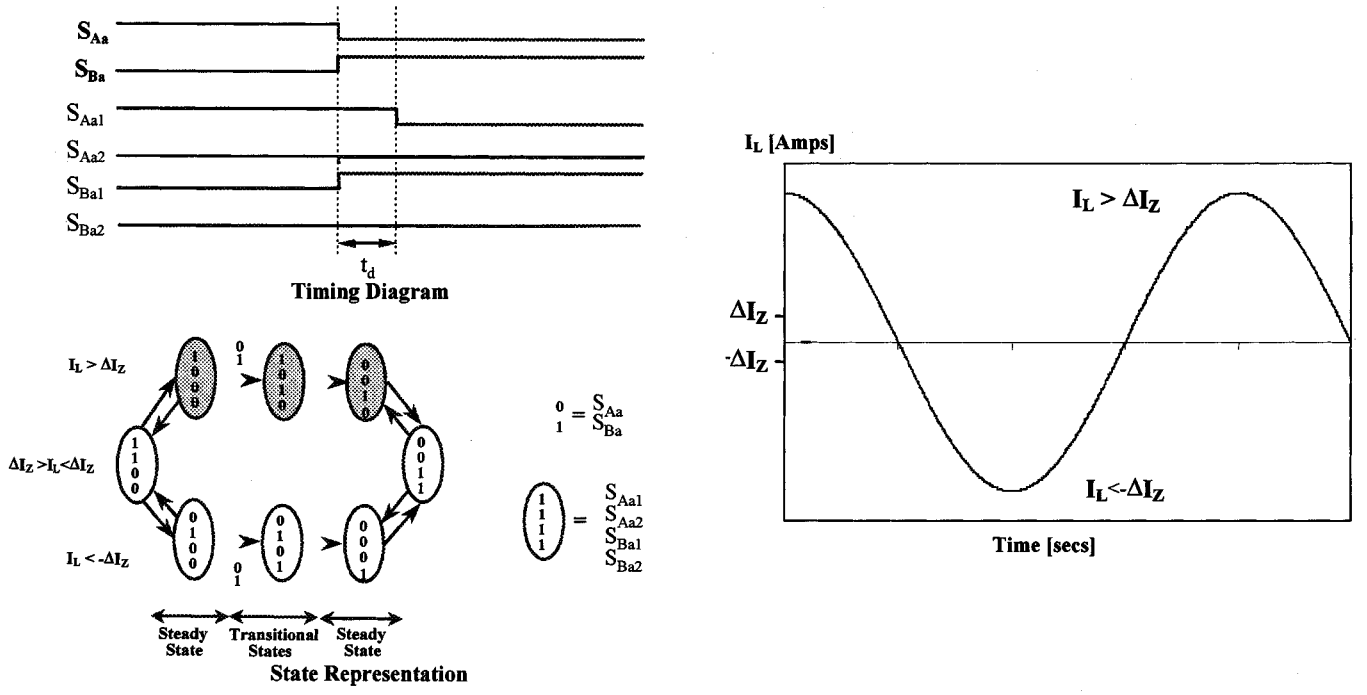

Fig. 11. Two-step semi-soft current commutation between two bidirectional switch cells.

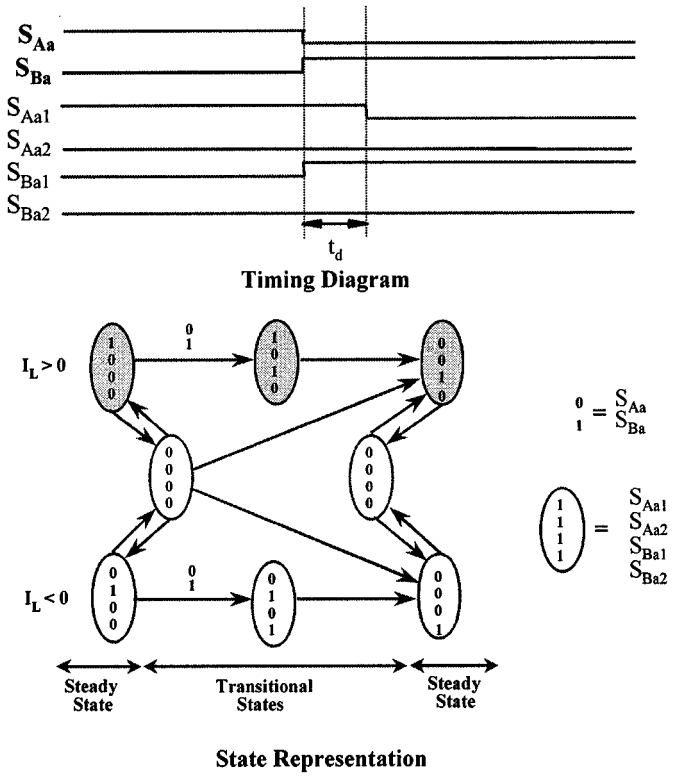

Fig. 12. Two-step semi-soft current commutation with current direction detection within the switch cell.

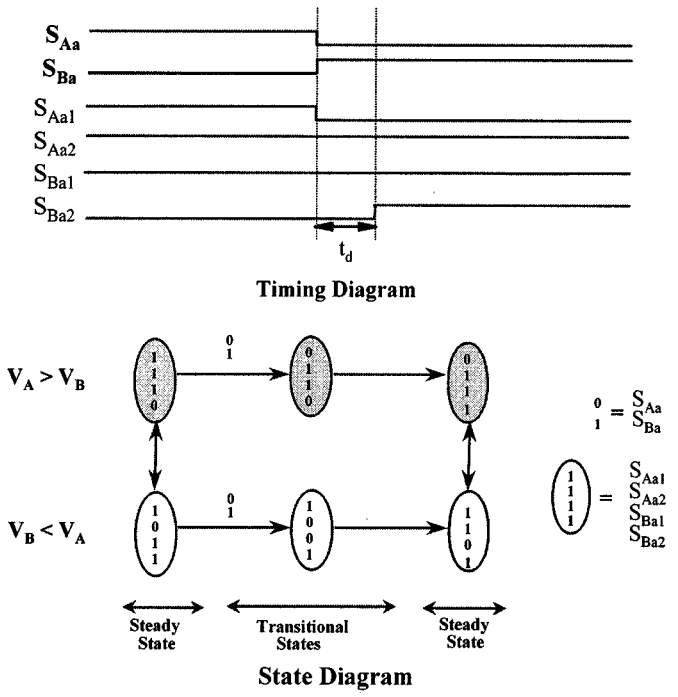

Fig. 13. Voltage-based current commutation.

V. Modulation Techniques

A. Basic Modulation Solution

The modulation problem normally considered for the matrix converter can be stated as follows.

Given a set of input voltages and an assumed set of output currents

$$\mathbf{v_i} = V_{im}\begin{bmatrix}\cos(\omega_i t)\\ \cos(\omega_i t + 2\pi/3)\\ \cos(\omega_i t + 4\pi/3)\end{bmatrix}$$

$$\mathbf{i_o} = I_{om}\begin{bmatrix}\cos(\omega_o t + \phi_o)\\ \cos(\omega_o t + \phi_o + 2\pi/3)\\ \cos(\omega_o t + \phi_o + 4\pi/3)\end{bmatrix} \tag{11}$$

find a modulation matrix $M(t)$ such that

$$\mathbf{v_o} = qV_{im}\begin{bmatrix}\cos(\omega_o t)\\ \cos(\omega_o t + 2\pi/3)\\ \cos(\omega_o t + 4\pi/3)\end{bmatrix}$$

and

$$\mathbf{i_i} = q\cos(\phi_o)I_{om}\begin{bmatrix}\cos(\omega_i t + \phi_i)\\ \cos(\omega_i t + \phi_i + 2\pi/3)\\ \cos(\omega_i t + \phi_i + 4\pi/3)\end{bmatrix} \quad (12)$$

and that the constraint equation (2) is satisfied. In (12), q is the voltage gain between the output and input voltages [10].

There are two basic solutions [10], [11], [54], as shown in (13) and (14) at the bottom of the page.

The solution in (13) yields $\phi_i = \phi_o$, giving the same phase displacement at the input and output ports, whereas the solution in (14) yields $\phi_i = -\phi_o$, giving reversed phase displacement. Combining the two solutions provides the means for input displacement factor control.

This basic solution represents a direct transfer function approach and is characterized by the fact that, during each switch sequence time (T_{seq}), the average output voltage is equal to the demand (target) voltage. For this to be possible, it is clear that the target voltages must fit within the input voltage envelope for any output frequency. This leads to a limitation on the maximum voltage ratio.

B. Voltage Ratio Limitation and Optimization

The modulation solutions in (13) and (14) have a maximum voltage ratio (q) of 50% as illustrated in Fig. 14.

An improvement in the achievable voltage ratio to $\sqrt{3}/2$ (or 87%) is possible by adding common-mode voltages to the target outputs as shown in (15)

$$\mathbf{v_o} = qV_{im} \cdot \begin{bmatrix}\cos(\omega_o t) - \frac{1}{6}\cos(3\omega_o t) + \frac{1}{2\sqrt{3}}\cos(3\omega_i t)\\ \cos(\omega_o t + 2\pi/3) - \frac{1}{6}\cos(3\omega_o t) + \frac{1}{2\sqrt{3}}\cos(3\omega_i t)\\ \cos(\omega_o t + 4\pi/3) - \frac{1}{6}\cos(3\omega_o t) + \frac{1}{2\sqrt{3}}\cos(3\omega_i t)\end{bmatrix}. \quad (15)$$

The common-mode voltages have no effect on the output line-to-line voltages, but allow the target outputs to fit within the input voltage envelope with a value of q up to 87% as illustrated in Fig. 15.

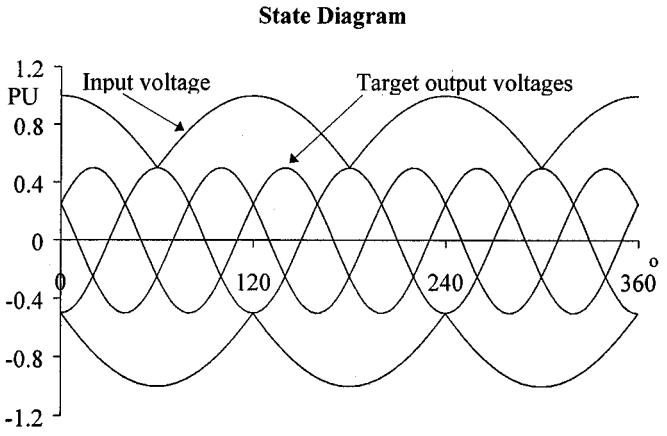

Fig. 14. Illustrating maximum voltage ratio of 50%.

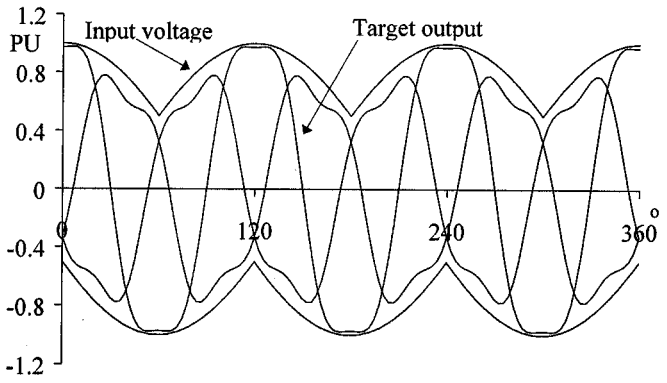

Fig. 15. Illustrating voltage ratio improvement to 87%.

The improvement in voltage ratio is achieved by redistributing the null output states of the converter (all output lines connected to the same input line) and is analogous to the similar well-established technique in conventional dc-link PWM converters. It should be noted that a voltage ratio of 87% is the intrinsic maximum for any modulation method where the target output voltage equals the mean output voltage during each switching sequence. Venturini provides a rigorous proof of this fact in [55] and [56].

C. Venturini Modulation Methods

The first method attributable to Venturini [10], [11], [54] is defined by (13) and (14). However, calculating the switch timings directly from these equations is cumbersome for a practical implementation. They are more conveniently expressed directly

$$\mathbf{M1} = \frac{1}{3}\begin{bmatrix}1+2q\cos(\omega_m t) & 1+2q\cos(\omega_m t - 2\pi/3) & 1+2q\cos(\omega_m t - 4\pi/3)\\ 1+2q\cos(\omega_m t - 4\pi/3) & 1+2q\cos(\omega_m t) & 1+2q\cos(\omega_m t - 2\pi/3)\\ 1+2q\cos(\omega_m t - 2\pi/3) & 1+2q\cos(\omega_m t - 4\pi/3) & 1+2q\cos(\omega_m t)\end{bmatrix}, \quad \text{with } \omega_m = (\omega_o - \omega_i) \quad (13)$$

$$\mathbf{M2} = \frac{1}{3}\begin{bmatrix}1+2q\cos(\omega_m t) & 1+2q\cos(\omega_m t - 2\pi/3) & 1+2q\cos(\omega_m t - 4\pi/3)\\ 1+2q\cos(\omega_m t - 2\pi/3) & 1+2q\cos(\omega_m t - 4\pi/3) & 1+2q\cos(\omega_m t)\\ 1+2q\cos(\omega_m t - 4\pi/3) & 1+2q\cos(\omega_m t) & 1+2q\cos(\omega_m t - 2\pi/3)\end{bmatrix}, \quad \text{with } \omega_m = -(\omega_o + \omega_i) \quad (14)$$

in terms of the input voltages and the target output voltages (assuming unity displacement factor) in the form of (16)

$$m_{Kj} = \frac{t_{Kj}}{T_{\text{seq}}} = \frac{1}{3}\left[1 + \frac{2v_K v_j}{V_{im}^2}\right] \quad \text{for } K = A, B, C \quad \text{and} \quad j = a, b, c. \tag{16}$$

This method is of little practical significance because of the 50% voltage ratio limitation.

Venturini's optimum method [55], [56] employs the common-mode addition technique defined in (15) to achieve a maximum voltage ratio of 87%. The formal statement of the algorithm, including displacement factor control, in Venturini's key paper [56] is rather complex and appears unsuited for real time implementation. In fact, if unity input displacement factor is required, then the algorithm can be more simply stated in the form of (17)

$$m_{Kj} = \frac{1}{3}\left[1 + \frac{2v_K v_j}{V_{im}^2} + \frac{4q}{3\sqrt{3}}\sin(\omega_i t + \beta_K)\sin(3\omega_i t)\right], \quad \text{for } K = A, B, C \quad \text{and} \quad j = a, b, c \quad \beta_K = 0, 2\pi/3, 4\pi/3 \quad \text{for } K = A, B, C, \text{ respectively.} \tag{17}$$

Note that, in (17), the target output voltages v_j include the common-mode addition defined in (15). Equation (17) provides a basis for real-time implementation of the optimum amplitude Venturini method which is readily handled by processors up to sequence (switching) frequencies of tens of kilohertz. Input displacement factor control can be introduced by inserting a phase shift between the measured input voltages and the voltages v_K inserted into (17). However, like all other methods, displacement factor control is at the expense of maximum voltage ratio.

Fig. 3 shown previously illustrates typical line to supply neutral output voltage and current waveforms generated by the Venturini method.

D. Scalar Modulation Methods

The "scalar" modulation method of Roy [57], [58] is typical of a number of modulation methods which have been developed where the switch actuation signals are calculated directly from measurements of the input voltages. The motivation behind their development is usually given as the perceived complexity of the Venturini method. The scalar method relies on measuring the instantaneous input voltages and comparing their relative magnitudes following the algorithm below.

Rule 1) Assign subscript M to the input which has a different polarity to the other two.

Rule 2) Assign subscript L to the smallest (absolute) of the other two inputs. Third input is assigned subscript K.

The modulation duty cycles are then given by

$$m_{Lj} = \frac{(v_j - v_M)v_L}{1.5V_{im}^2}$$
$$m_{Kj} = \frac{(v_j - v_M)v_K}{1.5V_{im}^2}$$
$$m_{Mj} = 1 - (m_{Lj} + m_{Kj}), \qquad \text{for } j = a, b, c. \tag{18}$$

Again, common-mode addition is used with the target output voltages v_j to achieve 87% voltage ratio capability.

Despite the apparent differences, this method yields virtually identical switch timings to the optimum Venturini method. Expressed in the form of (17), the modulation duty cycles for the scalar method are given in (19)

$$m_{Kj} = \frac{1}{3}\left[1 + \frac{2v_K v_j}{V_{im}^2} + \frac{2}{3}\sin(\omega_i t + \beta_K)\sin(3\omega_i t)\right]. \tag{19}$$

At maximum output voltage ($q = \sqrt{3}/2$), (17) and (19) are identical. The only difference between the methods is that the rightmost term addition is taken pro rata with q in the Venturini method and is fixed at its maximum value in the scalar method. The effect on output voltage quality is negligible except at low switching frequencies where the Venturini method is superior.

E. SPVM Methods

The SPVM is well known and established in conventional PWM inverters. Its application to matrix converters is conceptually the same, but is more complex [41]–[43], [45]. With a matrix converter, the SPVM can be applied to output voltage and input current control. A comprehensive discussion of the SPVM and its relationship to other methods is provided in [49]. Here, we just consider output voltage control to establish the basic principles.

The voltage space vector of the target matrix converter output voltages is defined in terms of the line-to-line voltages by (20)

$$\mathbf{V}_o(t) = \tfrac{2}{3}(v_{ab} + a v_{bc} + a^2 v_{ca}), \qquad \text{where } a = \exp(j2\pi/3). \tag{20}$$

In the complex plane, $\mathbf{V}_o(t)$ is a vector of constant length ($\sqrt{3}qV_{im}$) rotating at angular frequency ω_o. In the SPVM, $\mathbf{V}_o(t)$ is synthesized by time averaging from a selection of adjacent vectors in the set of converter output vectors in each sampling period. For a matrix converter, the selection of vectors is by no means unique and a number of possibilities exist which are not discussed in detail here.

The 27 possible output vectors for a three-phase matrix converter can be classified into three groups with the following characteristics.

- *Group I:* Each output line is connected to a different input line. Output space vectors are constant in amplitude, rotating (in either direction) at the supply angular frequency.
- *Group II:* Two output lines are connected to a common input line; the remaining output line is connected to one of the other input lines. Output space vectors have varying amplitude and fixed direction occupying one of six positions regularly spaced 60° apart. The maximum length of these vectors is $2/\sqrt{3}V_{env}$ where V_{env} is the instantaneous value of the rectified input voltage envelope.
- *Group III:* All output lines are connected to a common input line. Output space vectors have zero amplitude (i.e., located at the origin).

In the SPVM, the Group I vectors are not used. The desired output is synthesized from the Group II active vectors and the Group III zero vectors. The hexagon of possible output vectors

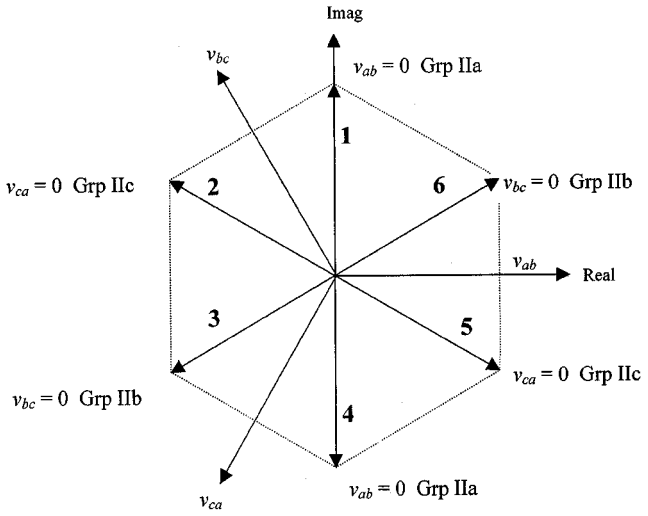

Fig. 16. Output voltage space vectors.

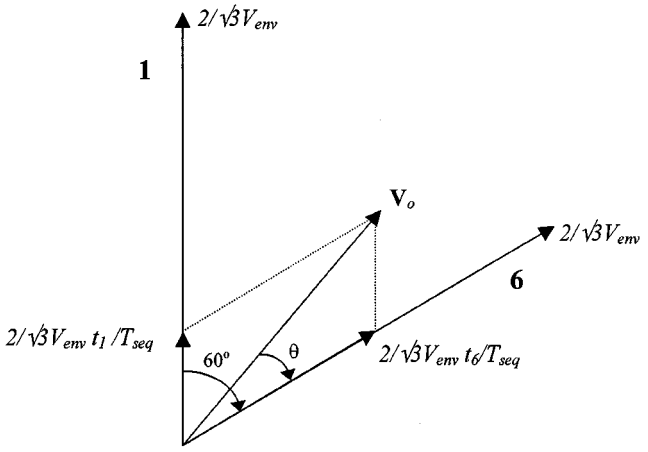

Fig. 17. Example of output voltage space-vector synthesis.

is shown in Fig. 16, where the Group II vectors are further subdivided dependent on which output line-to-line voltage is zero.

Fig. 17 shows an example of how $\mathbf{V}_o(t)$ could be synthesized when it lies in the sextant between vector 1 and vector 6. $\mathbf{V}_o(t)$ is generated through time averaging by choosing the time spent in vector 1 (t_1) and vector 6 (t_6) during the switching sequence. Here, it is assumed that the maximum length vectors are used, although that does not have to be the case. From Fig. 17, the relationship in (21) is found

$$\begin{aligned} t_1 &= \frac{|\mathbf{V}_o|}{V_{env}} T_{\text{seq}} \sin(\theta) \\ t_6 &= \frac{|\mathbf{V}_o|}{V_{env}} T_{\text{seq}} \sin(60 - \theta) \\ t_0 &= T_{\text{seq}} - (t_1 + t_6) \end{aligned} \tag{21}$$

where t_0 is the time spent in the zero vector (at the origin).

There is no unique way for distributing the times (t_1, t_6, t_0) within the switching sequence. One possible method is shown in Fig. 18.

For good harmonic performance at the input and output ports, it is necessary to apply the SPVM to input current control and

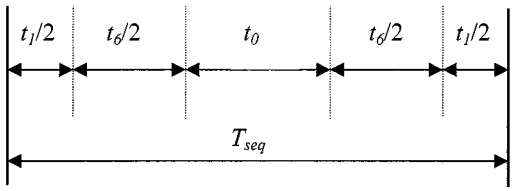

Fig. 18. Possible way of allocating states within switching sequence.

output voltage control. This generally requires four active vectors in each switching sequence, but the concept is the same. Under balanced input and output conditions, the SPVM technique yields similar results to the other methods mentioned earlier. However, the increased flexibility in choice of switching vectors for both input current and output voltage control can yield useful advantages under unbalanced conditions.

F. Indirect Modulation Methods

These methods aim to increase the maximum voltage ratio above the 86.6% limit of other methods [13], [40]. To do this, the modulation process defined in (9) is split into two steps as indicated in (22)

$$\mathbf{v_o} = (\mathbf{A}\mathbf{v_i})\mathbf{B}. \tag{22}$$

In (22), premultiplication of the input voltages by $\mathbf{A}$ generates a "fictitious dc link" and postmultiplication by $\mathbf{B}$ generates the desired output by modulating the "fictitious dc link." $\mathbf{A}$ is generally referred to as the "rectifier transformation" and $\mathbf{B}$ as the "inverter transformation" due to the similarity in concept with a traditional rectifier/dc link/inverter system. $\mathbf{A}$ is given by (23)

$$\mathbf{A} = K_A \begin{bmatrix} \cos(\omega_i t) \\ \cos(\omega_i t + 2\pi/3) \\ \cos(\omega_i t + 4\pi/3) \end{bmatrix}^T. \tag{23}$$

Hence,

$$\begin{aligned} \mathbf{A}\mathbf{v_i} &= K_A V_{im} \begin{bmatrix} \cos(\omega_i t) \\ \cos(\omega_i t + 2\pi/3) \\ \cos(\omega_i t + 4\pi/3) \end{bmatrix}^T \begin{bmatrix} \cos(\omega_i t) \\ \cos(\omega_i t + 2\pi/3) \\ \cos(\omega_i t + 4\pi/3) \end{bmatrix} \\ &= \frac{3K_A V_{im}}{2}. \end{aligned} \tag{24}$$

$\mathbf{B}$ is given by (25)

$$\mathbf{B} = K_B \begin{bmatrix} \cos(\omega_o t) \\ \cos(\omega_o t + 2\pi/3) \\ \cos(\omega_o t + 4\pi/3) \end{bmatrix}. \tag{25}$$

Hence,

$$\mathbf{v_o} = (\mathbf{A}\mathbf{v_i})\mathbf{B} = \frac{3K_A K_B V_{im}}{2} \begin{bmatrix} \cos(\omega_o t) \\ \cos(\omega_o t + 2\pi/3) \\ \cos(\omega_o t + 4\pi/3) \end{bmatrix}. \tag{26}$$

The voltage ratio $q = 3K_A K_B/2$. Clearly, the $\mathbf{A}$ and $\mathbf{B}$ modulation steps are not continuous in time as shown above, but must be implemented by a suitable choice of the switching states. There are many ways of doing this, which are discussed in detail in [13] and [40].

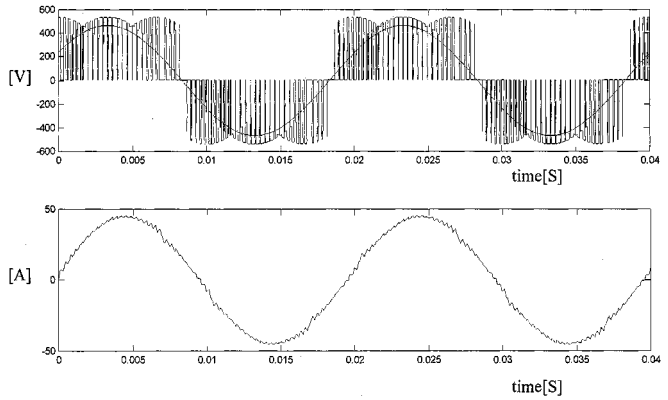

Fig. 19. Line-to-line voltage and current in the load with the indirect method. Output frequency of 50 Hz.

To maximize the voltage ratio, the step in $\mathbf{A}$ is implemented so that the most positive and most negative input voltages are selected continuously. This yields $K_A = 2\sqrt{3}/\pi$ with a "fictitious dc link" of $3\sqrt{3}V_{im}/\pi$ (the same as a six-pulse diode bridge with resistive load). K_B represents the modulation index of a PWM process and has the maximum value (square-wave modulation) of $2/\pi$ [13]. The overall voltage ratio q therefore has the maximum value of $6\sqrt{3}/\pi^2 = 105.3\%$.

The voltage ratio obtainable is obviously greater than that of other methods but the improvement is only obtained at the expense of the quality of either the input currents, the output voltages or both. For values of $q > 0.866$, the mean output voltage no longer equals the target output voltage in each switching interval. This inevitably leads to low frequency distortion in the output voltage and/or the input current compared to other methods with $q < 0.866$. For $q < 0.866$, the indirect method yields very similar results to the direct methods.

Fig. 19 shows typical line-to-line output voltage and current waveforms obtained with the indirect method generating an output voltage with a frequency of 50 Hz.

VI. Practical Issues

A. Input Filters

Filters must be used at the input of the matrix converters to reduce the switching frequency harmonics present in the input current. The requirements for the filter are [30] as follows:

1) to have a cutoff frequency lower than the switching frequency of the converter;
2) to minimize its reactive power at the grid frequency;
3) to minimize the volume and weight for capacitors and chokes;
4) to minimize the filter inductance voltage drop at rated current in order to avoid a reduction in the voltage transfer ratio.

It must be noticed that this filter does not need to store energy coming from the load. Several filter configurations like simple *LC* and multistage *LC* have been investigated [29]. It has been shown that simple *LC* filtering, as shown in Fig. 20, is the best alternative considering cost and size [29], [30].

The matrix converter is expected to be the "pure silicon converter," because it does not need large reactive elements to store energy. However, a recent study revealed that a matrix converter of 4 kW needed a larger volume for reactive components than a comparable dc-link inverter [30], although this solution had not been optimized for volume. Some preliminary research works have been reported concerning the size reduction of the input filter [25].

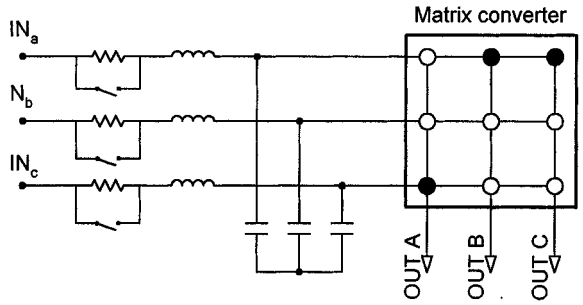

Fig. 20. Matrix converter with *LC* filter.

Due to the *LC* configuration of the input filter, some problems appear during the power-up procedure of the matrix converter. It is well known that an *LC* circuit can create overvoltage during transient operation. The connection of damping resistors, as shown in Fig. 20, to reduce overvoltages is proposed in [31]. The damping resistors are short circuited when the converter is running. The use of damping resistors connected in parallel to the input reactors is proposed in [30].

B. Overvoltage Protection

In a matrix converter, overvoltages can appear from the input side, originated by line perturbations. Also, dangerous overvoltages can appear from the output side, caused by an overcurrent fault. When the switches are turned off, the current in the load is suddenly interrupted. The energy stored in the motor inductance has to be discharged without creating dangerous overvoltages. A clamp circuit, as shown in Fig. 21, is the most common solution to avoid overvoltages coming from the grid and from the motor [32]. This clamp configuration uses 12 fast-recovery diodes to connect the capacitor to the input and output terminals.

A new clamp configuration uses six diodes from the bidirectional switches to reduce the extra diodes to six [23]. A different overvoltage protection strategy replaces the clamp by varistors connected at the input and at the output terminals, plus a simple extra circuit to protect each IGBT [24].

In [33], controlled shutdown of the converter without using a clamp is proposed. This strategy uses controlled freewheeling states to reduce the motor current to zero, avoiding the generation of overvoltages.

C. Ride-Through Capability

Ride-through capabability is a desired characteristic in modern drives [34], [35]. A common solution is to decelerate the drive during power loss, receiving energy from the load inertia to feed the control electronics and to magnetize the motor. This is achieved by maintaining a constant voltage in the dc-link capacitor. Matrix converters do not have a dc-link capacitor and, for this reason, the previously mentioned strategy cannot be used.

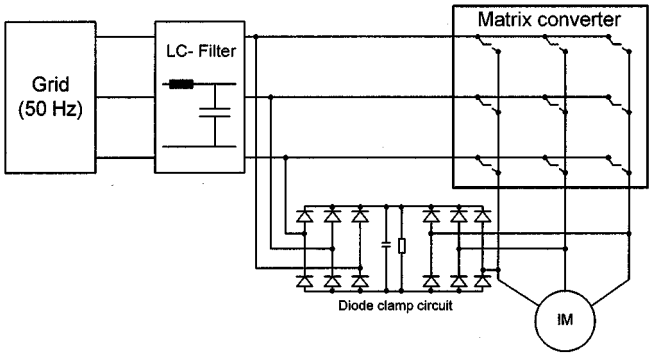

Fig. 21. Matrix converter with clamp.

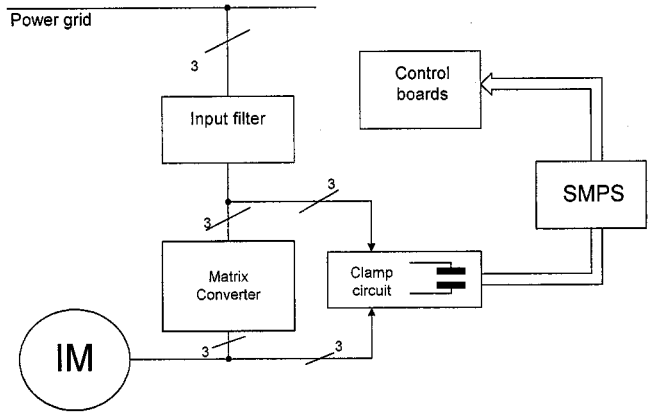

Fig. 22. Configuration to achieve ride-through capability.

Fig. 22 shows a configuration proposed to provide short-term ride-through capability to a matrix converter using the clamp capacitor as the source for a switch-mode power supply which feeds the converter control circuit [28]. After detection of a perturbation in the power supply, the motor is disconnected from the grid, but the switches of the matrix converter do not interrupt the motor currents. By applying the zero voltage vector (short circuit of the motor leads), the stator currents and the energy stored in the leakage inductance increases. The disconnection of the active switches originates the conduction of the clamp capacitor. This energy is then used to feed the control circuits. A flux and speed observer is used to restart the drive from nonzero flux and speed conditions in the shortest time.

VII. Comments and Conclusions

After two decades of research effort, several modulation and control methods have been developed for the matrix converter, allowing the generation of sinusoidal input and output currents, operating with unity power factor using standard processors. The most important practical implementation problem in the matrix converter circuit, the commutation problem between two controlled bidirectional switches, has been solved with the development of highly intelligent multistep commutation strategies. The solution to this problem has been made possible by using powerful digital devices that are now readily available in the market.

Another important drawback that has been present in all evaluations of matrix converters was the lack of a suitably packaged bidirectional switch and the large number of power semiconductors. This limitation has recently been overcome with the introduction of power modules which include the complete power circuit of the matrix converter. However, research work has shown that the matrix converter is not a "pure silicon converter" and that passive elements in the form of input filters are needed. More work must be done in order to optimize the size of these filters.

Twenty years ago, the matrix converter had the potential to be a superior converter in terms of its performance. Now, the matrix converter faces a very strong competition from the VSI with a three-phase active front end (AFE). This fully regenerative VSI-AFE topology has similar operating characteristics of sinusoidal input and output currents and adjustable power factor. In addition, the technology is mature and well established in the market. The real challenge for the matrix converter is to be accepted in the market. In order to achieve this goal, the matrix converter must overcome the VSI-AFE solution in terms of costs, size, and reliability.

References

[1] L. Gyugi and B. Pelly, *Static Power Frequency Changers: Theory, Performance and Applications*. New York: Wiley, 1976.
[2] A. Brandt, "Der Netztaktumrichter," *Bull. ASE*, vol. 62, no. 15, pp. 714–727, July 1971.
[3] W. Popov, "Der Direktumrichter mit zyklischer Steuerung," *Elektrie*, vol. 29, no. 7, pp. 372–376, 1975.
[4] E. Stacey, "An unrestricted frequency changer employing force commutated thyristors," in *Proc. IEEE PESC'76*, 1976, pp. 165–173.
[5] V. Jones and B. Bose, "A frequency step-up cycloconverter using power transistors in inverse-series mode," *Int. J. Electron.*, vol. 41, no. 6, pp. 573–587, 1976.
[6] M. Steinfels and P. Ecklebe, "Mit Direktumrichter Gespeiste Drehstromantriebe für den Industriellen Einsatz in einem Weiten Leistungsbereich," *Elektrie*, vol. 34, no. 5, pp. 238–240, 1980.
[7] P. Ecklebe, "Transistorisierter Direktumrichter für Drehstromantriebe," *Elektrie*, vol. 34, no. 8, pp. 413–433, 1980.
[8] A. Daniels and D. Slattery, "New power converter technique employing power transistors," *Proc. Inst. Elect. Eng.*, vol. 125, no. 2, pp. 146–150, Feb. 1978.
[9] ——, "Application of power transistors to polyphase regenerative power converters," *Proc. Inst. Elect. Eng.*, vol. 125, no. 7, pp. 643–647, July 1978.
[10] M. Venturini, "A new sine wave in sine wave out, conversion technique which eliminates reactive elements," in *Proc. POWERCON 7*, 1980, pp. E3_1–E3_15.
[11] M. Venturini and A. Alesina, "The generalized transformer: A new bidirectional sinusoidal waveform frequency converter with continuously adjustable input power factor," in *Proc. IEEE PESC'80*, 1980, pp. 242–252.
[12] J. Rodriguez, "A new control technique for AC–AC converters," in *Proc. IFAC Control in Power Electronics and Electrical Drives Conf.*, Lausanne, Switzerland, 1983, pp. 203–208.
[13] P. D. Ziogas, S. I. Khan, and M. H. Rashid, "Analysis and design of forced commutated cycloconverter structures with improved transfer characteristics," *IEEE Trans. Ind. Electron.*, vol. IE-33, pp. 271–280, Aug. 1986.
[14] L. Huber, D. Borojevic, and N. Burany, "Voltage space vector based PWM control of forced commutated cycloconvertors," in *Proc. IEEE IECON'89*, 1989, pp. 106–111.
[15] J. Oyama, T. Higuchi, E. Yamada, T. Koga, and T. Lipo, "New control strategy for matrix converter," in *Proc. IEEE PESC'89*, 1989, pp. 360–367.

[16] M. Braun and K. Hasse, "A direct frequency changer with control of input reactive power," in *Proc. IFAC Control in Power Electronics and Electrical Drives Conf.*, Lausanne, Switzerland, 1983, pp. 187–194.
[17] E. Wiechmann, J. Espinoza, L. Salazar, and J. Rodriguez, "A direct frequency converter controlled by space vectors," in *Proc. IEEE PESC'93*, 1993, pp. 314–320.
[18] G. Kastner and J. Rodriguez, "A forced commutated cycloconverter with control of the source and load currents," in *Proc. EPE'85*, 1985, pp. 1141–1146.
[19] C. L. Neft and C. D. Schauder, "Theory and design of a 30-HP matrix converter," *IEEE Trans. Ind. Applicat.*, vol. 28, pp. 546–551, May/June 1992.
[20] J. H. Youm and B. H. Kwon, "Switching technique for current-controlled AC-to-AC converters," *IEEE Trans. Ind. Electron.*, vol. 46, pp. 309–318, Apr. 1999.
[21] L. Empringham, P. Wheeler, and J. Clare, "Intelligent commutation of matrix converter bi-directional switch cells using novel gate drive techniques," in *Proc. IEEE PESC'98*, 1998, pp. 707–713.
[22] M. Ziegler and W. Hofmann, "Performance of a two steps commutated matrix converter for ac-variable-speed drives," in *Proc. EPE'99*, 1999, CD-ROM.
[23] P. Nielsen, F. Blaabjerg, and J. Pedersen, "Novel solutions for protection of matrix converter to three phase induction machine," in *Conf. Rec. IEEE-IAS Annu. Meeting*, 1997, pp. 1447–1454.
[24] J. Mahlein and M. Braun, "A matrix converter without diode clamped over-voltage protection," in *Proc. IPEMC 2000*, Beijing, China, pp. 817–822.
[25] C. Klumpner, P. Nielsen, I. Boldea, and F. Blaabjerg, "New steps toward a low-cost power electronic building block for matrix converters," in *Conf. Rec. IEEE-IAS Annu. Meeting*, 2000, CD-ROM.
[26] J. Chang, T. Sun, A. Wang, and D. Braun, "Medium power AC–AC converter based on integrated bidirectional power modules, adaptive commutation and DSP control," in *Conf. Rec. IEEE-IAS Annu. Meeting*, 1999, CD-ROM.
[27] D. Casadei, G. Serra, A. Tani, and P. Nielsen, "Theoretical and experimental analysis os SVM-controlled matrix converters under unbalanced supply conditions," *Electromotion*, vol. 4, pp. 28–37, 1997.
[28] C. Klumpner, I. Boldea, and F. Blaabjerg, "Short term ride through capabilities for direct frequency converters," in *Conf. Rec. IEEE PESC'00*, 2000, CD-ROM.
[29] P. Wheeler, H. Zhang, and D. Grant, "A theoretical and practical consideration of optimized input filter design for a low loss matrix converter," in *Proc. IEE PEVD Conf.*, Sept. 1994, pp. 363–367.
[30] C. Klumpner, P. Nielsen, I. Boldea, and F. Blaabjerg, "A new matrix converter-motor (MCM) for industry applications," in *Conf. Rec. IEEE-IAS Annu. Meeting*, 2000, CD-ROM.
[31] C. Klumpner and F. Blaabjerg, "The matrix converter: overvoltages caused by the input filter, bidirectional power flow, and control for artificial loading of induction motors," *Elect. Mach. Power Syst.*, vol. 28, pp. 129–242, 2000.
[32] C. L. Neft, "AC power supplied static switching apparatus having energy recovery capability," U.S. Patent 4 697 230, 1987.
[33] A. Shuster, "A matrix converter without reactive clamp elements for an induction motor drive system," in *Proc. IEEE PESC'98*, 1998, pp. 714–720.
[34] J. Holtz and W. Lotzkat, "Controlled AC drives with ride-through capability at power interruption," *IEEE Trans. Ind. Applicat.*, vol. 30, pp. 1275–1283, Sept./Oct. 1994.
[35] A. Von Jouanne, P. Enjeti, and B. Banerjee, "Assessment of ride-through alternatives for adjustable speed drives," in *Conf. Rec. IEEE-IAS Annu. Meeting*, 1998, pp. 1538–1545.
[36] N. Burany, "Safe control of four-quadrant switches," in *Conf. Rec. IEEE-IAS Annu. Meeting*, 1989, pp. 1190–1194.
[37] M. Ziegler and W. Hofmann, "Semi natural two steps commutation strategy for matrix converters," in *Proc. IEEE PESC'98*, 1998, pp. 727–731.
[38] L. Empringham, P. Wheeler, and J. Clare, "Bi-directional switch current commutation for matrix converter applications," in *Proc. PEMatrix Converter Prague*, Sept. 1998, pp. 42–47.
[39] ——, "Matrix converter bi-directional switch commutation using intelligent gate drives," in *Proc. IEE PEVD Conf.*, London, U.K., 1998, pp. 626–631.
[40] P. Ziogas, S. Khan, and M. Rashid, "Some improved forced commutated cycloconverter structures," *IEEE Trans. Ind. Applicat.*, vol. 1A-21, pp. 1242–1253, Sept./Oct. 1985.
[41] L. Huber and D. Borojevic, "Space vector modulator for forced commutated cycloconverters," in *Conf. Rec. IEEE-IAS Annu. Meeting*, 1989, pp. 871–876.
[42] L. Huber, D. Borojevic, and N. Burany, "Analysis design and implementation of the space-vector modulator for forced-commutated cycloconvertors," *Proc. Inst. Elect. Eng.*, pt. B, vol. 139, no. 2, pp. 103–113, Mar. 1992.
[43] L. Huber, D. Borojevic, X. Zhuang, and F. Lee, "Design and implementation of a three-phase to three-phase matrix converter with input power factor correction," in *Proc. IEEE APEC'93*, 1993, pp. 860–865.
[44] L. Huber, D. Borojevic, and N. Burany, "Digital implementation of the space vector modulator for forced commutated cycloconverters," in *Proc. IEE PEVD Conf.*, 1990, pp. 63–65.
[45] L. Huber and D. Borojevic, "Space vector modulated three phase to three phase matrix converter with input power factor correction," *IEEE Trans. Ind. Applicat.*, vol. 31, pp. 1234–1246, Nov./Dec. 1995.
[46] P. Wheeler and D. Grant, "Optimized input filter design and low loss switching techniques for a practical matrix converter," *Proc. Inst. Elect. Eng.*, pt. B, vol. 144, no. 1, pp. 53–60, Jan. 1997.
[47] M. Munzer, "EconoMac—The first all in one IGBT module for matrix converters," in *Proc. Drives and Control Conf.*, sec. 3, London, U.K., 2001, CD-ROM.
[48] T. Svensson and M. Alakula, "The modulation and control of a matrix converter synchronous machine drive," in *Proc. EPE'91*, Florence, Italy, 1991, pp. 469–476.
[49] D. Casadei, G. Serra, A. Tani, and L. Zarri, "Matrix converter modulation strategies: A new general approach based on space-vector representation of the switch state," *IEEE Trans. Ind. Electron.*, vol. 49, pp. 370–381, Apr. 2002.
[50] B. H. Kwon, B. H. Min, and J. H. Kim, "Novel commutation technique of AC–AC converters," *Proc. Inst. Elect. Eng.*, pt. B, pp. 295–300, July 1998.
[51] C. T. Pan, T. C. Chen, and J. J. Shieh, "A zero switching loss matrix converter," in *Proc. IEEE PESC'93*, 1993, pp. 545–550.
[52] M. V. M. Villaça and A. J. Perin, "A soft switched direct frequency changer," in *Conf. Rec. IEEE-IAS Annu. Meeting*, 1995, pp. 2321–2326.
[53] J. G. Cho and G. H. Cho, "Soft switched matrix converter for high frequency direct AC-to-AC power conversion," in *Proc. EPE'91*, Florence, Italy, 1991, pp. 4-196–4-201.
[54] A. Alesina and M. G. B. Venturini, "Solid-state power conversion: A Fourier analysis approach to generalized transformer synthesis," *IEEE Trans. Circuits Syst.*, vol. CAS-28, pp. 319–330, Apr. 1981.
[55] A. Alesina and M. Venturini, "Intrinsic amplitude limits and optimum design of 9-switches direct PWM AC–AC converters," in *Proc. IEEE PESC'88*, vol. Apr., 1988, pp. 1284–1291.
[56] A. Alesina and M. G. B. Venturini, "Analysis and design of optimum-amplitude nine-switch direct AC–AC converters," *IEEE Trans. Power Electron.*, vol. 4, pp. 101–112, Jan. 1989.
[57] G. Roy, L. Duguay, S. Manias, and G. E. April, "Asynchronous operation of cycloconverter with improved voltage gain by employing a scalar control algorithm," in *Conf. Rec. IEEE-IAS Annu. Meeting*, 1987, pp. 889–898.
[58] G. Roy and G. E. April, "Cycloconverter operation under a new scalar control algorithm," in *Proc. IEEE PESC'89*, 1989, pp. 368–375.

Patrick W. Wheeler (M'00) received the Ph.D. degree in electrical engineering from the University of Bristol, Bristol, U.K., in 1993.

In 1993, he joined the University of Nottingham, Nottingham, U.K., as a Research Assistant in the Department of Electrical and Electronic Engineering, where, since 1996, he has been a Lecturer in Power Electronic Systems in the Power Electronics, Machines and Control Group. His research interests are variable-speed ac motor drives, in particular, different circuit topologies, power converters for power systems, and semiconductor switch use.

Dr. Wheeler is a member of the Institution of Electrical Engineers, U.K.

José Rodríguez (M'81–SM'94) received the Engineer degree from the University Técnica Federico Santa María, Valparaiso, Chile, and the Dr.-Ing. degree from the University of Erlangen, Erlangen, Germany, in 1977 and 1985, respectively, both in electrical engineering.

Since 1977, he has been with the University Técnica Federico Santa María, where he is currently a Professor and Head of the Department of Electronic Engineering. During his sabbatical leave in 1996, he was responsible for the Mining Division of Siemens Corporation in Chile. He has extensive consulting experience in the mining industry, especially in the application of large drives like cycloconverter-fed synchronous motors for SAG mills, high-power conveyors, controlled drives for shovels, and power quality issues. His research interests are mainly in the areas of power electronics and electrical drives. Recently, his main research interests have been multilevel inverters and new converter topologies. He has authored or coauthored more than 100 refereed journal and conference papers and contributed to one chapter in *Power Electronics Handbook* (New York: Academic, 2001).

Jon C. Clare (M'90) was born in Bristol, U.K., in 1957. He received the B.Sc. and Ph.D. degrees in electrical engineering from the University of Bristol, Bristol, U.K.

From 1984 to 1990, he was a Research Assistant and Lecturer at the University of Bristol, involved in teaching and research in power electronic systems. Since 1990, he has been with the Power Electronics, Machines and Control Group, School of Electrical and Electronic Engineering, University of Nottingham, Nottingham, U.K., where he is currently a Senior Lecturer in Power Electronics. His research interests are power electronic converters and modulation strategies, variable-speed drive systems, and electromagnetic compatibility.

Dr. Clare is a member of the Institution of Electrical Engineers, U.K.

Lee Empringham (M'00) received the B.Eng. (hons) degree in electrical and electronic engineering and the Ph.D. degree from the University of Nottingham, Nottingham, U.K., in 1996 and 2000, respectively.

He joined the Power Electronics, Machines and Control Group, School of Electrical and Electronic Engineering, University of Nottingham, to work on matrix converter commutation techniques. He is currently a Research Assistant in the group, supporting different ongoing matrix converter projects. His research interests include direct ac–ac power conversion, variable-speed ac motor drives using different circuit topologies, and more-electric/electric automobiles.

Dr. L. Empringham is a member of the Institution of Electrical Engineers, U.K.

Alejandro Weinstein is working toward the Masters degree in the Departamento de Electronica, Universidad Técnica Federico Santa María, Valparaiso, Chile.

He is also an Electronic Engineer in the Departamento de Electronica, Universidad Técnica Federico Santa María.